XLVI CILAMCE
VITÓRIA - ES - BRAZIL - 2025
XLVI IBERO-LATIN AMERICAN CONGRESS ON COMPUTATIONAL METHODS IN ENGINEERING

Analysis of welded connections between thin-walled circular hollow section (CHS) columns and I-section beams formed by cold-formed steel (CFS) profiles

Ladir A. Silva Junior[1], Matheus M. Oliveira[1], Vinícius N. Alves[1], Arlene M. C. Sarmanho[1]

[1]*Dept. of Civil Engineering, University of Ouro Preto*
Rua Professor Paulo Magalhães Gomes, 122, 35400-000, Ouro Preto – MG, Brazil
ladir.junior@aluno.ufop.edu.br, matheusmoliveira4@gmail.com, vinicius.alves@ufop.edu.br, arlene@ufop.edu.br

Abstract. This study investigates the behavior of welded T-joint connections between thin-walled circular hollow section (CHS) columns and I-section beams fabricated from cold-formed steel (CFS) profiles. The research addresses the lack of national and international standards specifically applicable to slender sections, which are widely used in Brazil due to less stringent environmental and load conditions. Numerical models were developed using the finite element method in ANSYS 18.2 and validated against experimental results from the literature. A parametric study involving 36 models investigated the influence of three key geometric parameters: column section slenderness (2γ), the ratio of beam flange width to column diameter (β), and the ratio of beam height to column diameter (η). The study included 16 models with CFS I-beams (double sections placed back-to-back) formed by plain channel C-sections, and 16 with lipped C-sections, focusing on moment resistance and initial rotational stiffness. The results revealed that current design formulations do not accurately predict the behavior of these connections. Beams formed with lipped C-sections exhibited an average increase of 15.9% in moment resistance and 16.8% in initial rotational stiffness compared to formed by plain channel C-sections. These findings underscore the need for further research on welded T-joints involving thin-walled CHS columns and cold-formed I-beams, highlighting the structural advantages of lipped C-sections in enhancing both strength and stiffness.

Keywords: Initial Rotational Stiffness; Finite Elements; Parametric Analysis; Welded Connections.

1 Introduction

Steel structures are a well-established and efficient solution in Brazilian civil construction, owing to their high strength-to-weight ratio, rapid construction, cost-effectiveness, and architectural versatility. Furthermore, industrialized fabrication enhances quality control and minimizes material waste, aligning with sustainability objectives.

Internationally, advancements in technology and design methodologies have enabled the development of complex steel structures, requiring structural systems capable of resisting torsion and biaxial bending [1]. In this context, Circular Hollow Sections (CHS) stand out due to their favorable mechanical performance, offering high resistance to compression, torsion, and bending and functional adaptability [1], [2].

A highly effective structural system combines CHS columns with I-section beams, leveraging the advantages of both cross-sectional profiles [3]. However, the performance of such systems is highly dependent on behavior of their connection, which governs structural strength, stiffness, and economic viability [4].

In Brazil, the demand for lightweight and rapidly assembled structures has driven the adoption of tubular sections. However, current standards lack provisions for slender-wall sections, despite their widespread use in national practice.

Although there are design formulations for connections between CHS columns and hot-rolled beams, studies involving thin-walled CHS columns and cold-formed steel (CFS) I-beams remain limited, despite the widespread use of these structural components in warehouses and medium-rise buildings. This study addresses this gap by investigating the structural behavior of welded T-joints connections between thin-walled CHS columns (Classes 3 and 4 [5]) and I-section beams composed of cold-formed plain channel or lipped C-sections. The research involves numerical modeling in ANSYS 18.2 [6], validated against experimental data from the literature, followed by a parametric study to evaluate their strength and initial rotational stiffness. The numerical results were compared with

existing equations in the literature.

2 Design standards for CHS column to I-section beam welded connections

International standards and design guides such as EN 1993-1-8 [7], NBR 16239 [8], CIDECT – Design Guide 1 [9], and ISO 14346 [10] provide methodologies for evaluating the strength of welded connections between CHS columns and I-section beams, considering the column face plastification failure mode. These documents are based on experimental data and analytical models that consider transverse plate behavior, incorporating correction factors and empirical expressions to account for geometric and material variability. Table 1 summarizes the design formulations for T-joint connections governed by column face plastification, as prescribed by these standards.

Table 1. Design formulations for plastification failure of the column face or cross-section

	NBR 16239 [8]	**ISO 14346 [10] CIDECT–1 [9]**	**EN 1993-1-8 [7]**
$\mathbf{M_{1.Rk}}$:	$Q_{ub} k_p f_{y0} t_0^2 h_1$	$Q_{ub} Q_f f_{y0} t_0^2 h_1$	$Q_{ub} Q_f C_f f_{y0} t_0^2 (h_1 - t_1)$
$\mathbf{Q_{ub}}$	$\frac{Q_u}{(1+0.25\eta)}$	$\frac{Q_u}{(1+0.4\eta)}$	$\frac{Q_u}{(1+0.4\eta)}$
$\mathbf{Q_{u,T}}$:	$4.0(1+5.0\beta^2)(1+0.25\eta)$	$2.2(1+6{,}8\beta^2)(1+0.4\eta)\gamma^{0,2}$	$2.3(1+3\beta^2)(1+0.4\eta)\gamma^{0.35}$

Where $M_{1.Rk}$ denotes the design moment resistance of the joint, Q_{ub} the reduction factor for bending, k_p a coefficient related to column stresses, f_{y0} the yield strength of the column , t_0 the column wall thickness, h_1 the depth of the I-section beam, Q_f the column stress function, C_f the material factor, t_1 the beam flange thickness, and Q_u the reduction factor for axial loading. The geometric parameters are defined as: $\eta=h_1/d_0$ (beam depth-to-column diameter ratio), $\beta=b_1/d_0$ (beam width-to-column diameter ratio), and $\gamma=d_0/2t_0$ (column diameter-to-thickness ratio).

To ensure structural safety and serviceability, these standards impose applicability limits based on geometric and material parameters. Key restrictions include limits on material yield strength, minimum tubular wall thickness, and geometric ratios (β, η and 2γ). Critically, these standards are limited to compact sections (Class 1 or 2 [5]), thereby excluding thin-walled sections (Classes 3 and 4 [5]). This limitation is significant for regions like Brazil, where slender sections are widely adopted due to lower structural demands and cost considerations. Thus, this study addresses a critical gap by investigating CHS-to-I beam connections with thin-walled columns, which are currently unaddressed by international standards.

2.1 Determination of Initial Rotational Stiffness

While international standards provide methods for assessing the resistance of welded CHS-to-I-beam connections with non-slender walls, they lack explicit procedures for estimating initial rotational stiffness. This gap has spurred significant research efforts to develop reliable stiffness prediction models.

Among relevant studies, the works of Kurobane et al. [11] and Di Benedetto et al. [12] stand out, having proposed equations to estimate the stiffness in welded T-joint connections between CHS columns and I-beams, as shown in Equations (1) and (2), respectively.

$$S_{i,Kurobane} = \frac{1.9\, E\, t_0\, (2\gamma)^{-0.7}\, (\beta)^{1.3}\, \left(h_1 - t_f\right)^2}{2} \tag{1}$$

Where E is the steel's modulus of elasticity, 2γ is the column diameter-to-thickness ratio (d_0/t_0), β is the ratio between the beam width and the column diameter (b_1/d_0), h1 is the beam height, and tf is the beam flange thickness.

$$S_{i,Benedetto} = \frac{E t_0 (h_b - t_{bf})^2}{\frac{4(1+\nu)}{\pi}\beta_\nu \eta + \frac{\gamma \xi_f}{a}} \tag{2}$$

Where hb is the beam height, tbf is the beam flange thickness, ν is Poisson's ratio, $\beta\nu$ is a reduction factor accounting for the beneficial effect of shear in the column, η is the ratio between beam height and column diameter (h_b/d_0), ξ_f denotes the ratio between the column thickness and the beam flange thickness (t_0/t_{bf}), and a is *a* coefficient calibrated from numerical results, taken as 1.33.

3 Materials and Methods

Finite element models were developed using ANSYS 18.2 [6] to analyze the structural performance of welded T-joints between CHS columns and cold-formed steel (CFS) I-beams. The numerical approach was first validated

against experimental data from Reis [2] for non-slender CHS columns (Classes 1 and 2). Following validation, a parametric study was conducted to evaluate the performance of connections involving thin-walled CHS columns (Classes 3 and 4), for which no experimental data exist, highlighting the relevance of the numerical approach adopted in this study.

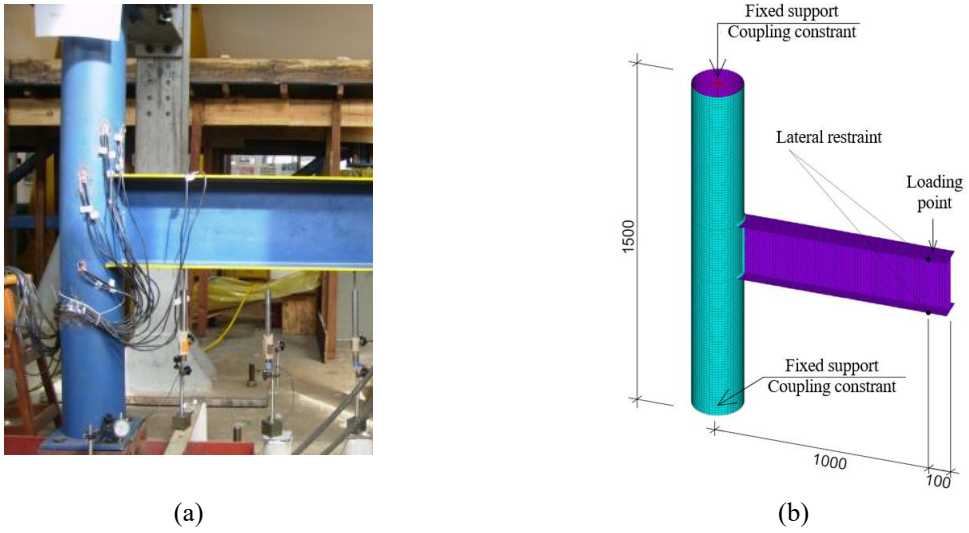
3.1 Finite Element Model

The numerical analysis was performed using the finite element method in ANSYS 18.2 [6], which is a widely used software in structural engineering research. A three-dimensional model of the CHS-to-I-beam T-joint was developed and validated against experimental data from Reis [2], specifically using two identical prototypes from their study. The geometric and material properties used for validation are summarized in Table 2.

Table 2. Geometric and material properties of experimental modes.

CHS Column			**I-Beam**					**Weld**	**Non-dimensional parameters**		
d_0 [mm]	t_0 [mm]	f_y [MPa]	h_1 [mm]	b_1 [mm]	t_f [mm]	t_w [mm]	f_y [MPa]	$a\sqrt{2}$ [mm]	β (b_1/d_0)	2γ (d_o/t_0)	η (h_1/d_0)
219.1	8.2	385.0	251.0	101.0	5.3	4.8	345.0	7.95	0.46	26.72	1.15

To replicate the experimental conditions of Reis et al. [2], the simulation employed a 1500 mm column with fixed ends and a 1100 mm I-beam. The model included lateral restraint at 1000 mm from the CHS axis and displacement loading at the same distance. All endpoints were fully constrained. Figure 1 shows the geometric characteristics of the models. Figure 2(a) presents the nomenclature and non-dimensional parameters for connections between CHS columns and I-beams.



(a) (b)

Figure 1. Geometric properties of the models: (a) experimental analysis, Reis [2]; (b) numerical models, dimensions in mm.

The analysis incorporated both geometric and material nonlinearities through a nonlinear static formulation. Material behavior was modeled an elastic-plastic model with linear strain hardening, as specified in EN 1993-1-5 [13]. The material properties adopted were: elastic modulus E = 200000 MPa , tangent modulus Et = E/100 [13], and Poisson's ratio of 0.3. Based on experimental data, the weld leg size was assumed to be constant at 7.95 mm. To ensure that failure occurred in the beam-to-column connection rather than in the weld itself, the weld material strength was increased to 2000 MPa.

SHELL181 elements, with four nodes and six degrees of freedom per node [6], were used to model both the column and the beam. The weld at the interface was modeled using SOLID185 elements, defined by eight nodes and three translational degrees of freedom (in x, y, and z directions) [6]. A uniform mesh size of 10 mm was applied, and loading was simulated by imposing displacements at a constant rate of 0.33 mm per substep. The nonlinear equations were solved using the Newton–Raphson iterative method. The analysis was terminated based on the deformation limit criterion proposed by Lu et al. [14], which defines the ultimate limit state as the point when the deformation of the column face exceeds 3% of the column diameter (d_0).

3.2 Validation

The validation procedure followed the methodology proposed by Lu et al. [14], where connection resistance was determined by: (a) the peak moment if it occurred before 3%·d₀ deformation, or (b) the minimum value between the moment at 3%·d₀ and 1.5 times the moment at 1%·d₀ if the peak occurred later.

The initial rotational stiffness was obtained using the secant method applied to the linear portion of the moment–rotation curve [11], [12]. Following Barros et al. [15], a reference rotation of 1/5 of 1%·d₀ was adopted. Elastic rotations from the beam and column were subtracted according to Equation (3):

$$\varphi_p = \varphi_t - \varphi_{e,c} - \varphi_{e,b} = \varphi_t - \frac{FL_b^2}{3EI_b} - \frac{ML_c}{16EI_c} \tag{3}$$

where φ_p represents the plastic rotation of the connection; φ_t denotes the total rotation, calculated as the ratio of the vertical displacement at the beam's end (actuator) to the beam length from the column axis to the actuator; $\varphi_{e,c}$ is the elastic rotation of the column; and $\varphi_{e,c}$is the elastic rotation of the beam. F is the force applied by the actuator at the beam's end, L_b is the beam length from the column axis to the actuator, E is the modulus of elasticity, I_b and I_c are the moments of inertia of the I-beam and the CHS column, respectively. M represents the bending moment generated by the actuator force relative to the column axis, and L_c is the total length of the column.

Figure 2(b) and Table 3 present the comparison between the numerical models and the experimental results for validation purposes.

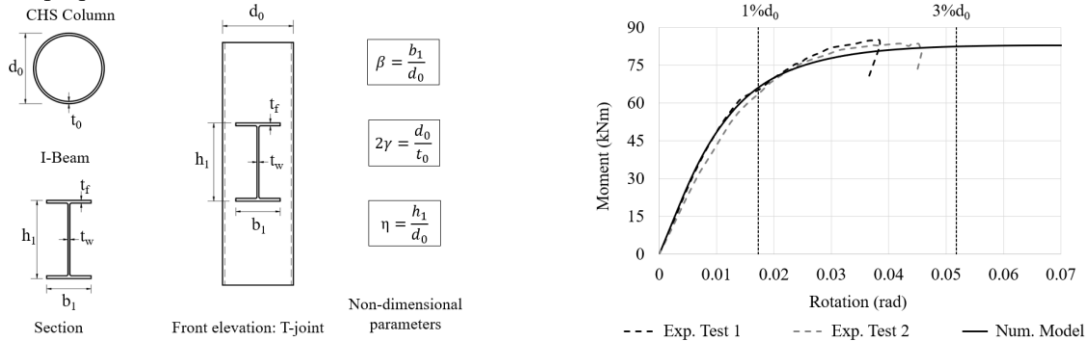


Figure 2. (a) Nomenclature and non-dimensional parameters for connections Between CHS Columns and I-Beams; (b) Experimental results versus FE results.

Table 3. Experimental results versus FE results.

Prototype	Serviceability Moment			Ultimate Moment			Initial rotational stiffness (φ_t)		
	Exp. Test [kN.m]	Num. Model [kN.m]	Error [%]	Exp. Test [kN.m]	Num. Model [kN.m]	Error [%]	Exp. Test [kN.m/rad]	Num. Model [kN.m/rad]	Error [%]
Reis - Test 1	65.06	66.53	2.26%	84.97	82.56	2.84%	5105.08	5274.54	3.32
Reis - Test 2	63.99	66.53	3.97%	83.62	82.56	1.27%	4798.93	5274.54	9.91

It can be observed that the numerical model accurately reproduced the experimental behavior reported by Reis [2]. For a reference rotation of 1% of the column diameter (d₀), the maximum difference between the numerical and experimental moment was 3.97%. Regarding the maximum resistant moment, the discrepancies were 2.84% for test 1 and 1.27% for test 2. In both cases, the peak moment was adopted as a reference, since the tests were interrupted before reaching the 3%·d₀ rotation limit. For the initial rotational stiffness, the maximum errors were 9.91% for test 2 and 3.32% for test 1. Based on the criterion proposed by Lu et al. [14], it is concluded that the Ultimate Limit State governs the connection's load-bearing capacity. The results confirm that the numerical model provides a reliable representation of the experimental behavior.

3.3 Parametric Analysis

A parametric study was conducted using on the validated numerical model from Section 2.2, assessing the behavior of welded beam-to-column connections between thin-walled CHS columns (Classes 3 and 4) and CFS I-section beams formed by either plain channel or lipped C-sections. The investigation focused on three primary parameters: column section slenderness (2γ), flange width-to-column diameter ratio (β), and beam height-to-column diameter ratio (η) (see Figure 2(a)).

For the CFS I-beams, an intermittent welding pattern along the web edges was adopted. In accordance with NBR 14762 [17], this approach maintains independent web behavior rather than creating a monolithic section. Thus, only a single web thickness was considered in the numerical models.

CHS columns with an external diameter (d_0) of 200 mm and wall thicknesses (t_0) of 3.00 mm and 3.75 mm were analyzed, corresponding to slender sections (Classes 3 or 4), with 2γ values exceeding the limits specified in EN 1993-1-8 [7]. Beams had heights (h_1) of 200 mm, 300 mm, and 400 mm, and flange widths (b_1) of 100 mm, 135 mm, and 170 mm, all with a constant thickness of 4.75 mm, classifying them as non-slender (Classes 1 or 2).

A total of 32 numerical models were developed, 16 models with CFS I-beams (double sections placed back-to-back) formed by plain channel C-sections, and 16 with lipped C-sections, covering β values from 0.50 to 0.85, η from 1.0 to 2.0, and 2γ from 53.33 to 66.67. Columns were modeled using Class C steel (f_y = 317 MPa) according to NBR 8261 [16], and beams with CIV 300 steel (f_y = 300 MPa). Weld leg size was set to 1.5 times t_0, in accordance with NBR 16239 [8], while other properties followed those of the validated model [2].

Figure 3 illustrates the geometric variations and model nomenclature, formatted $d_0_t_0_b_1_h_1_(i)$, where (i) denotes the beam type – either plain channel or lipped C-sections. A 25 mm edge stiffener was incorporated in all models using back-to-back lipped C-sections.

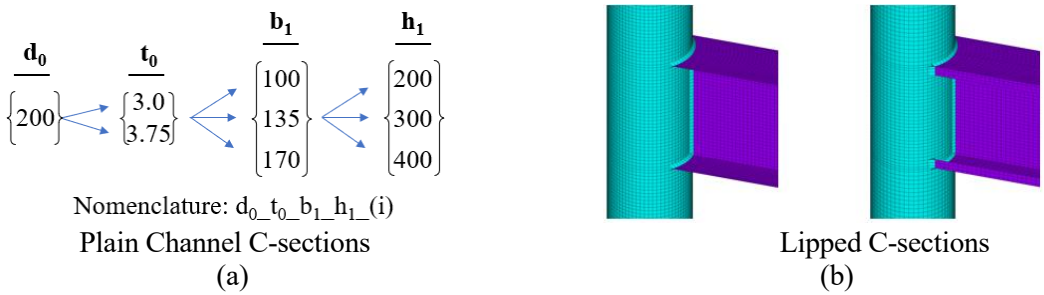


Figure 3. Geometric variations in the parametric study: (a) Geometric configurations and adopted nomenclature; (b) Detailed view of the numerical models.

4 Results and Discussion

The bending moments obtained from the numerical models developed in the parametric were compared with the theoretical formulations proposed by NBR 16239 [8], ISO 14346 [10], and EN 1993-1-8 [7], to evaluate their agreement with the simulated results regarding connection strength. For consistency, design values were adopted across all standards. The results are presented in Table 4.

Table 4. Summary of parametric study results – Moment resistance.

Prototype	FE results			NBR 16239 [8]			ISO 14346 [10]			EN 1993-1-8 [7]		
$d_0_t_0_b_1_h_1_(i)$	$M_{r,U,}$ [kN.m]	$M_{r,C}$ [kN.m]	$\frac{M_{r,C}}{M_{r,U}}$	M_{1rd} [kN.m]	$\frac{M_{1rd}}{M_{r,U\,num}}$	$\frac{M_{1rd}}{M_{r,C\,num}}$	M_{1rd} [kN.m]	$\frac{M_{1rd}}{M_{r,U\,num}}$	$\frac{M_{1rd}}{M_{r,C\,num}}$	M_{1rd} [kN.m]	$\frac{M_{1rd}}{M_{r,U\,num}}$	$\frac{M_{1rd}}{M_{r,C\,num}}$
200_3.75_100_200_(i)	16.22	19.33	1.19	8.02	0.49	0.41	10.21	0.63	0.53	11.06	0.68	0.57
200_3.75_100_300_(i)	23.47	27.7	1.18	12.04	0.51	0.43	15.32	0.65	0.55	16.72	0.71	0.6
200_3.75_100_400_(i)	31.57	36.28	1.15	16.05	0.51	0.44	20.42	0.65	0.56	22.38	0.71	0.62
200_3.75_135_200_(i)	24.38	29.11	1.19	11.69	0.48	0.4	15.68	0.64	0.54	15.08	0.62	0.52
200_3.75_135_300_(i)	35.06	40.74	1.16	17.54	0.5	0.43	23.51	0.67	0.58	22.8	0.65	0.56
200_3.75_135_400_(i)	45.72	52.46	1.15	23.38	0.51	0.45	31.35	0.69	0.6	30.53	0.67	0.58
200_3.75_170_200_(i)	37.34	45.5	1.22	16.45	0.44	0.36	22.37	0.6	0.49	20.01	0.54	0.44
200_3.75_170_300_(i)	53.8	63.89	1.19	24.67	0.46	0.39	33.55	0.62	0.53	30.26	0.56	0.47
200_3.75_170_400_(i)	68.82	80.59	1.17	32.9	0.48	0.41	44.73	0.65	0.56	40.51	0.59	0.5
200_3.00_100_200_(i)	11.25	13.02	1.16	5.14	0.46	0.39	6.83	0.61	0.52	7.65	0.68	0.59
200_3.00_100_300_(i)	16.22	18.36	1.13	7.7	0.47	0.42	10.25	0.63	0.56	11.57	0.71	0.63
200_3.00_100_400_(i)	21.63	23.91	1.11	10.27	0.47	0.43	13.67	0.63	0.57	15.49	0.72	0.65
200_3.00_135_200_(i)	17.39	20.21	1.16	7.48	0.43	0.37	10.37	0.6	0.51	10.35	0.6	0.51
200_3.00_135_300_(i)	24.73	27.96	1.13	11.22	0.45	0.4	15.56	0.63	0.56	15.65	0.63	0.56
200_3.00_135_400_(i)	32.03	35.85	1.12	14.96	0.47	0.42	20.75	0.65	0.58	20.95	0.65	0.58
200_3.00_170_200_(i)	27	31.83	1.18	10.53	0.39	0.33	14.97	0.55	0.47	13.85	0.51	0.44
200_3.00_170_300_(i)	38.69	44.5	1.15	15.79	0.41	0.35	22.45	0.58	0.5	20.94	0.54	0.47
200_3.00_170_400_(i)	49.23	55.83	1.13	21.06	0.43	0.38	29.93	0.61	0.54	28.03	0.57	0.50
Mean			1.16		0.47	0.40		0.63	0.54		0.64	0.54
Coefficient of Variation (CoV - %)			2.46		7.31	8.06		4.96	6.09		10.18	11.92

The numerical models produced higher moment resistance than those predicted by the design standards. Increases in the geometric parameters β and η resulted in greater moment resistance, while higher values of 2γ led to a reduction. Models using I-beams formed by lipped C-sections consistently outperformed those with plain channel C-sections, with an average strength gain of 15.94% and a coefficient of variation (CoV) of 2.46%.

None of the evaluated standards adequately represented the behavior of connections with thin-walled CHS columns (Classes 3 and 4), systematically underestimating the resistance for both beam types. NBR 16239 [8] showed the weakest correlation, with an average ratio of 0.40 between code-based and numerical results for lipped C-section beams (CoV: 8.06%). Conversely, EN 1993-1-8 [7] yielded the best estimates for plain channel C-section beams, with an average ratio of 0.64 and CoV of 10.18%. Importantly, none of the analytical models considered the beneficial stiffening effect introduced by the lipped C-section geometry.

The initial rotational stiffness from the numerical models was evaluated against the analytical expressions proposed by Kurobane et al. [11] and Di Benedetto et al. [12], to assess the compatibility of these formulations with the observed numerical behavior. The results are presented in Table 5.

Table 4. Summary of parametric study results – Initial rotational stiffness.

Prototype	**Numerical results**			**Benedetto *et al.* [12]**			**Kurobane *et al.*** [11]		
$d_0_t_0_b_1_h_1_(i)$	$k_{U,\,num}$ [kN.m/rad]	$K_{C,\,num}$ [kN.m/rad]	$\frac{k_C}{k_U}$	$K_{Ben.}$ [kN.m/rad]	$\frac{k_{Ben.}}{k_{U,num}}$	$\frac{k_{Ben.}}{k_{C,num}}$	$K_{Kur.}$ [kN.m/rad]	$\frac{k_{Kur.}}{k_{U,num}}$	$\frac{k_{Kur.}}{k_{C,num}}$
200_3.75_100_200_(i)	1485.24	1747.83	1.18	1658.96	1.12	0.95	681.91	0.46	0.39
200_3.75_100_300_(i)	2481.74	2889.84	1.16	3675.31	1.48	1.27	1559.29	0.63	0.54
200_3.75_100_400_(i)	3702.93	4279.16	1.16	6426.3	1.74	1.50	2794.41	0.75	0.65
200_3.75_135_200_(i)	2233.99	2631.6	1.18	1658.96	0.74	0.63	1017.02	0.46	0.39
200_3.75_135_300_(i)	3653.82	4267.1	1.17	3675.31	1.01	0.86	2325.56	0.64	0.54
200_3.75_135_400_(i)	5380.82	6242.83	1.16	6426.3	1.19	1.03	4167.65	0.77	0.67
200_3.75_170_200_(i)	3302.55	3923.83	1.19	1659.48	0.50	0.42	1359.29	0.41	0.35
200_3.75_170_300_(i)	5355.49	6330.13	1.18	3676.34	0.69	0.58	3108.21	0.58	0.49
200_3.75_170_400_(i)	7827.79	9197.59	1.17	6427.9	0.82	0.70	5570.24	0.71	0.61
200_3.00_100_200_(i)	1050.9	1223.63	1.16	1327.58	1.26	1.08	466.64	0.44	0.38
200_ 3.00_100_300_(i)	1747.9	2017.47	1.15	2941.07	1.68	1.46	1067.04	0.61	0.53
200_ 3.00_100_400_(i)	2608.08	2990.78	1.15	5142.32	1.97	1.72	1912.24	0.73	0.64
200_ 3.00_135_200_(i)	1637.35	1916.32	1.17	1327.58	0.81	0.69	689.31	0.42	0.36
200_ 3.00_135_300_(i)	2662.9	3087.15	1.16	2941.07	1.10	0.95	1576.21	0.59	0.51
200_ 3.00_135_400_(i)	3909.86	4504.54	1.15	5142.32	1.32	1.14	2824.73	0.72	0.63
200_ 3.00_170_200_(i)	2539.45	3009.8	1.19	1327.58	0.52	0.44	930.18	0.37	0.31
200_ 3.00_170_300_(i)	4071.83	4782.68	1.17	2941.07	0.72	0.61	2126.98	0.52	0.44
200_ 3.00_170_400_(i)	5909.94	6903.69	1.17	5142.32	0.87	0.74	3811.77	0.64	0.55
Mean			1.17		1.09	0.93		0.58	0.50
Coefficient of Variation (CoV - %)			0.98		39.20	40.10		22.51	23.19

As expected, the rotational stiffness behavior followed the same trends as the moment resistance. Increases in β and η led to greater initial stiffness, while higher 2γ values resulted in reduced stiffness. Models with lipped C-section beams showed, on average, 16.79% higher stiffness than those with plain channel C-sections, with a low CoV of 0.98%.

For plain channel C-section beams, the formulation by Di Benedetto et al. [12] produced an average analytical-to-numerical stiffness ratio of 1.09 (CoV: 39.20%), indicating significant variability despite a close mean. For lipped C-section beams, the average ratio was 0.93 with a CoV of 40.10%, reinforcing the limited predictive accuracy of the formulation, likely due to the omission of the β parameter.

The model proposed by Kurobane et al. [11] also underestimated stiffness values, yielding an average ratio of 0.58 for plain channel C-section beams (CoV: 22.51%) and 0.50 for lipped C-section beams (CoV: 23.19%). These findings confirm that current equations are inadequate for capturing the stiffness behavior of connections involving thin-walled CHS columns and cold-formed I-section beams.

5 Conclusion

This study evaluated the structural performance of welded T-joint connections between thin-walled CHS columns (Class 3 and 4) and I-section beams formed by cold-formed plain channel and lipped C-sections. Numerical simulations, validated against experimental data, revealed that existing design standards (NBR 16239, ISO 14346

and EN 1993-1-8) significantly underestimate the moment capacity and rotational stiffness of such connections, particularly due to the absence of formulations suited for slender-wall components.

Beams formed by lipped C-sections demonstrated superior structural behavior, with increases of approximately 16% in both moment resistance and initial rotational stiffness compared to plain channel C-section beams. The parametric analysis also highlighted the influence of geometric parameters β, η, and 2γ on connection performance.

These findings point to the need for revising existing formulations to better account for slender-walled elements and for incorporating parameters such as β in stiffness prediction models. Furthermore, experimental investigations are recommended to deepen the understanding of these connections, especially considering that current literature does not address welded joints involving thin-walled CHS columns and cold-formed C-section beams.

Acknowledgments

The authors gratefully acknowledge the support from the FAPEMIG (Minas Gerais State Research Support Foundation), CAPES (Higher Education Personnel Improvement Coordination), CNPq (National Council for Scientific and Technological Development), and UFOP (Federal University of Ouro Preto), including the Propec (Civil Engineering Postgraduate Program).

References

[1] J. Wardenier, J. A. Packer, X.-L. Zhao, and G. J. van der VEGTE, "*Hollow sections in structural applications*". Comité International pour le Développement et l'Etude de la Construction Tubulaire - CIDECT, 2a ed., 2010.
[2] S. L. F. Reis, "*Análise teórico-experimental de ligações metálicas soldadas entre coluna em perfil tubular circular e viga em perfil de seção transversal 'I'*". Universidade de Ouro Preto, Master's Dissertation, Ouro Preto, 2011.
[3] M. A. Serrano-López, C. López-Colina, Y. C. Wang, M. Lozano, I. García, and F. L. Gayarre, "An experimental study of I beam-RHS column demountable joints with welded studs," *J Constr Steel Res*, vol. 182, Jul. 2021, doi: 10.1016/j.jcsr.2021.106651.
[4] A. H. M. de Araújo, A. M. Sarmanho, E. de M. Batista, J. A. V. Requena, R. H. Fakury, and R. J. Pimenta, "*Projeto de Estruturas de Edificações com Perfis Tubulares de Aço*", vol. 1. Belo Horizonte: Rona Editora LTDA, 2016.
[5] EN 1993-1-1, "Eurocode 3: Design of steel structures - Part 1-1: General principles and principles for buildings". Brussels, Belgium: CEN (European Commitee for Standardization), 2024.
[6] ANSYS Inc., "ANSYS," 2017, EUA: Swanson Analysis System: 18.2.
[7] EN 1993-1-8, "Eurocode 3: Design of steel structures - Part 1-8: Design of joints. Brussels", Belgium: CEN (European Commitee for Standardization), 2024.
[8] Associação Brasileira de Normas Técnicas (ABNT), "NBR 16239: Projeto de estruturas de aço e de estruturas mistas de aço e concreto de edificações com perfis tubulares". 2013.
[9] J. Wardenier, Y. Kurobane, J. A. Packer, G. J. Van Der Vegte, and X.-L. Zhao, *"Design Guide 1: Design guide for Circular Hollow Section (CHS) joints under predominantly static loading"*. CIDECT - Constrution With Hollow Steel Sections, Genebra, 2008.
[10] ISO 14346, "Static design procedure for welded hollow-section joints - Recommendations". INTERNATIONAL STANDARD, 2013, p. 52.
[11] Y. Kurobane, J. A. Packer, J. Wardenier, and N. Yeomans, "*Design Guide 9: For structural hollow section column connections*". CIDECT - Constrution with Hollow Steel Sections, TÜV-Verlag, 2004, p. 211.
[12] S. Di Benedetto, M. Latour, and G. Rizzano, "Stiffness prediction of connections between CHS tubes and externally welded I-beams: Fe analyses and analytical study," *Materials*, vol. 13, no. 13, Jul. 2020, doi: 10.3390/ma13133030.
[13] EN 1993-1-5, "Eurocode 3: Design of steel structures - Part 1-5: Plated structural elements". Brussels, Belgium: CEN (European Commitee for Standardization), 2024.
[14] L. H. Lu, G. D. de Winkel, Y. Yu, and J. Wardenier, "Deformation limit for the strength of hollow section joints," *Tubular Structures VI*, pp. 341–347, 1994.
[15] H. T. G. de Barros, M. M. de Oliveira, A. M. C. Sarmanho, and V. N. Alves, "Stiffness assessment of welded I-beam to RHS column connections," *Eng Struct*, vol. 267, Sep. 2022, doi: 10.1016/j.engstruct.2022.114661.
[16] Associação Brasileira de Normas Técnicas (ABNT), "NBR 8261: Tubos de aço-carbono, com e sem solda, de seção circular, quadrada ou retangular para usos estruturais — Requisitos". 2019.
[17] Associação Brasileira de Normas Técnicas (ABNT), "NBR 14762: Dimensionamento de estruturas de aço constituídas por perfis formados a frio", 2010.